CONF-961200--88 ANL/CMT/CP--90407

CHARACTERIZATION OF A PU-BEARING ZIRCONOLITE-RICH SYNROC

E. C. Buck, B. Ebbinghaus,* A. J. Bakel, and J. K. Bates

Chemical Technology Division
ARGONNE NATIONAL LABORATORY
9700 South Cass Avenue
Argonne, IL 60439-4837

*Lawrence Livermore National Laboratory
P. O. Box 808
Livermore, CA 94550

Submitted to

1996 Fall Meeting
Materials Research Society
Boston, MA
December 2-5, 1996

This work was supported by the U.S. Department of Energy, Office of Fissile Materials Disposition, under contract W-31-109-ENG-38.

DISCLAIMER

CHARACTERIZATION OF A PU-BEARING ZIRCONOLITE-RICH SYNROC

E. C. BUCK, B. EBBINGHAUS,* A. J . BAKEL, and J. K. BATES
Argonne National Laboratory, Argonne, IL 60439
*Lawrence Livermore National Laboratory, Livermore, CA 94550

ABSTRACT

A titanate-based ceramic waste form, rich in phases structurally related to zirconolite ($CaZrTi_2O_7$), is being developed as a possible method for immobilizing excess plutonium from dismantled nuclear weapons. As part of this program, Lawrence Livermore National Laboratory (LLNL) produced several ceramics that were then characterized at Argonne National Laboratory (ANL). The plutonium-loaded ceramic was found to contain a Pu-Gd zirconolite phase but also contained plutonium titanates, Gd-polymignyte, and a series of other phases. In addition, much of the Pu was remained as PuO_{2-x}. The Pu oxidation state in the zirconolite was determined to be mainly Pu^{4+}, although some Pu^{3+} was believed to be present.

INTRODUCTION

Titanium minerals such as rutile, ilmenite ($FeTiO_3$), and arizonite (Fe_2TiO_5) are extremely insoluble in water, and therefore varieties of titanate-based mineral phases (or Synrocs) have been studied for some time as possible nuclear waste storage materials [1-4]. Evidence from the laboratory testing and from the study of natural analogues of the constituent phases of Synroc suggests that these materials are extremely corrosion resistant [1-3]. Recently, zirconolite-rich ceramics have been considered for the disposal of actinide-bearing waste streams, in particular excess Pu from dismantled nuclear weapons [5]. However, the heterogeneous nature of Synroc waste forms may make it difficult to predict the long-term behavior of these types of materials.

In this paper we report on the production and microstructural characterization of a preliminary Fissile Materials Disposition (MD) ceramic formulation which has been designed for high-Pu loadings. The purpose of this study is to obtain data to support the choice of a waste form for Pu immobilization. The data presented in this paper are only preliminary, as the MD ceramic composition has not, as yet, been finalized.

EXPERIMENTAL PROCEDURES

Preparation of the Pu-Loaded Ceramic

The plutonium oxide (PuO_{2-x}) used to prepare the Pu-loaded ceramic at LLNL was made from a low temperature (<200°C) oxidation of $PuH_{2.7}$ in a 4% O_2/Ar atmosphere. The hydride was formed at about 100°C from a weapons Pu pit. The PuO_2 was split into two batches: half was calcined at 450°C for four hours (low fired) and half was calcined at 1000°C for four hours (high fired). The PuO_2 particles ranged in size from 20 μm to about 100 μm, with an average at around 65 μm.

The ceramic material was prepared by two different methods. In one series of samples the precursor material was made from precipitation of alkoxides, with the Gd_2O_3 (the low energy neutron absorber) and PuO_2 added as powders in a wet slurry. This material was then dried and calcined at 750°C for about 4 hours. In another series, the precursor material which was ground, dried, pulverized, and then calcined at 600°C for 1 hour, consisted of $Zr(NO_3)_4 \cdot 5H_2O$, TiO_2, Gd_2O_3, CaO, $Al(OH)_3$, and BaO. The product was dry blended with PuO_2 in a mortar and pestle. The blended powder was cold pressed at 1055 kg/cm^2 in a 1.27 cm stainless steel die to produce green pellets. These pellets were sintered at 1325°C for 1-4 hours. The target compositions for the Pu-loaded ceramic materials are presented in Table I.

Table I. Target Composition of Pu-Loaded Ceramic Material
(values reported in wt%)

PuO_x Calcine Conditions Prep. Route	Low-Fired, Hot-Pressed Alkoxides	High-Fired, Hot-Pressed Alkoxide	High-Fired, Cold-Pressed Oxides
CaO	7.3	6.5	8.1
ZrO_2	16.1	14.4	17.7
TiO_2	38.6	34.4	40.4
Al_2O_3	10.9	9.7	4.7
BaO	3.0	2.7	3.4
PuO_2	14.4	19.3	16.9
Gd_2O_3	9.6	12.9	8.7

Methods for Characterization

Scanning electron microscopy (SEM) analyses were performed at ANL on an ISI microscope with a backscattered electron detector. Representative particles of the material, around 5-30 μm in diameter, were selected with the aid of an optical microscope and embedded into epoxy blocks. Thin sections of the MD ceramic were produced with an ultramicrotome from the blocks; these thin sections were suitable for transmission electron microscopy (TEM). Phase characterizations were performed with a JEOL 2000 FXII TEM, operating at 200 kV, which was equipped with an X-ray energy dispersive spectrometer (EDS) and parallel electron energy loss spectrometer. Several zone axis patterns were used to determine the structure of each phase encountered. The camera lengths for electron diffraction were calibrated with a polycrystalline aluminum sample. Compositional analysis was achieved with TEM/EDS while remaining off the Bragg angle to avoid electron beam channeling.

Leach Test Procedure

Static leach tests were carried out in accordance with the PCT-A procedure [6]. Crushed ceramic (-100+200 mesh) was prepared and examined with SEM to verify the absence of fines. Approximately 1 g of the crushed ceramic and 10 g of deionized water (ASTM-1) were placed in a 22 mL stainless steel (Type 304) Parr vessel. The surface-area-to-solution-volume (S/V) ratio of the PCT-A test is assumed to be around 2000 m^{-1} for a material with a density of 2.7 g/cm^3. Since the ceramic used in these tests has a higher density (4.7 g/cm^3), the actual S/V of these tests is significantly less than 2000 m^{-1}. The vessels were sealed with a Teflon gasket and placed in a 90°C (± 2°C) oven for 7 days along with an experimental blank test. At the end of the test period, the leachates were analyzed for pH and cation concentrations and the reacted material was examined with SEM. The insides of the vessels were soaked in 2% HNO_3 for 8 hours, and the "acid strip" solution was collected and analyzed for cations. The cation concentrations from the leachates and the "acid strip" solutions were summed to calculate normalized mass losses. Previously determined background values were subtracted from the cation concentrations.

Vapor Hydration Testing

Sample discs were prepared by cutting ~1 x 10 mm wafers from the MD ceramic and polishing the discs to a 600 grit finish. The wafers were suspended via Pt-Rh wires inside a Parr vessel. Sufficient deionized water was added to saturate the air inside the vessel once it had been sealed and at the set temperature. Diagrams of the apparatus have been presented elsewhere [7]. The tests were conducted at 200°C for up to 91 days. After test termination the vessel was examined with SEM and TEM.

MICROSTRUCTURAL CHARACTERIZATION

Ceramic waste forms designed for Pu immobilization are composed of at least 80% zirconolite and pyrochlore phases [5]. Zirconolite has the highest durability of the all the phases in Synroc and is capable of accepting into its structure a variety of ions. The grain size of the ceramic was generally <1 μm, which meant that we were unable to distinguish individual phases with the SEM (see Fig. 1). Therefore, phase characterizations were performed with the analytical TEM. Although the major titanate-based phases are well known, waste loadings can induce the formation of unique phases, which may not be visible with X-ray diffraction (XRD). In the MD ceramic, the high concentration of Pu and Gd may also induce the formation of different phases. Based on SEM examination, it was clear that the ceramic contained a substantial amount of undissolved PuO_2 (see Fig. 1). This result was expected, due to the large PuO_2 particle size used. The material that was characterized was a mixture of the compositions described in Table I.

Zirconolite and Related Structures

The major phase observed in the ceramic was a Pu- and Gd-bearing zirconolite phase, containing nearly equal amounts of Pu and Gd in the structure. Gadolinium-rich phases, identified as being closely related to polymignyte, were also found in the ceramic. With electron energy loss spectroscopy (EELS), we were able to demonstrate the presence of a trace amount of Ce, possibly an impurity in the added Gd, in the zirconolite phase (see Figs. 2a-c).

Zirconolite does not always incorporate radionuclides by isomorphic substitution. Rather, distinct phases form as a consequence of particular elements present in the waste [8]. Radioactive elements are not distributed uniformly throughout the material but concentrated in extended defects [7]. It is most constructive to consider the zirconolite and related structures in terms of layered hexagonal tungsten bronze (HTB) motifs [8]. The repeating unit can be observed in high-resolution images of zirconolite (see Fig. 2d).

The diffraction patterns from these phases can be interpreted in terms of the stacking of the HTB which allows easy comparison of the various zirconolite polytypes. Using procedures developed by White for HTB arrangements [8], it is possible to interpret the electron diffraction patterns of zirconolite polytypes without the need for high resolution imaging. These methods were used to understand the nature of the zirconolite phases formed in the Pu-ceramic formulation. The diffraction pattern of a zirconolite polytype is shown in Fig. 3a.

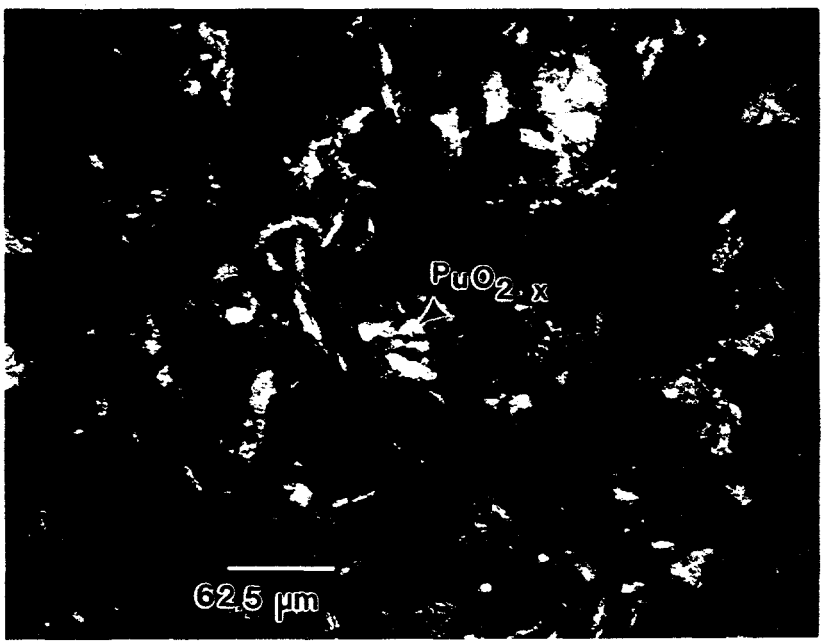

Fig. 1. Backscattered SEM Image of the Surface of the Pu-Ceramic which was Formed with High-Fired PuO_{2-x} and Hot Pressed at 1275°C for 1 hr. The material is porous and shows the presence of undissolved plutonium oxide (bright contrast). The porous regions may contribute to increased levels of release.

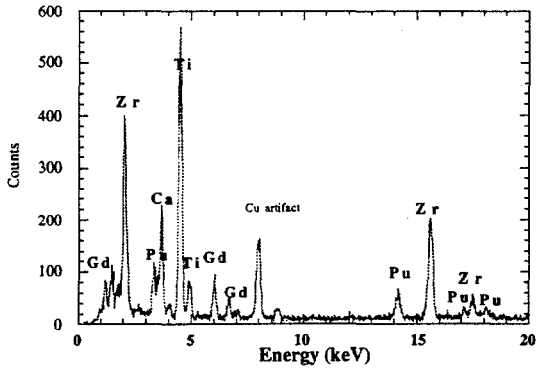

Fig. 2a. EDS Analysis of Pu-Gd Zirconolite.

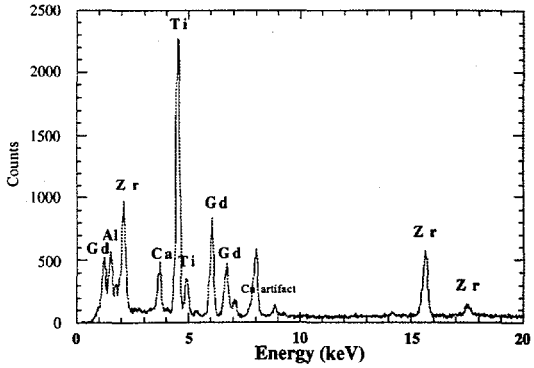

Fig. 2b. EDS Analysis of Gd-Pyrochlore Phase.

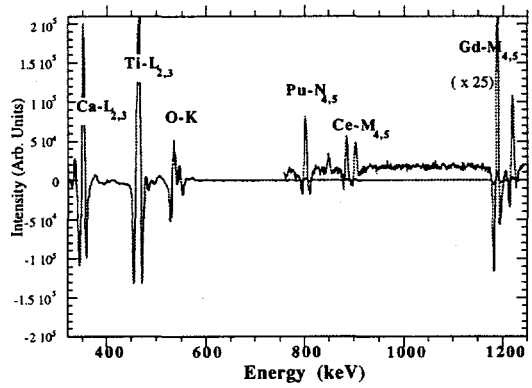

Fig. 2c. TEM/EELS of Zirconolite Phase Showing the Presence of a Trace Amount of Ce. The spectrum collected is the second derivative which helps to reveal some of the finer features of the spectrum.

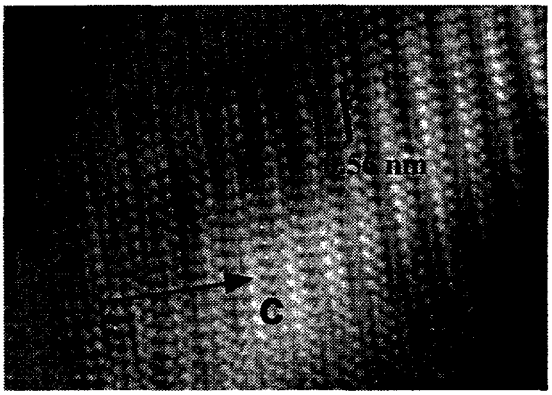

Fig. 2d. Fourier Filtered Multibeam Image of Zirconolite Phase. As described by White [7], the stacking of HTB layers results in bimodular repeat with **c*** = ~1.11 nm.

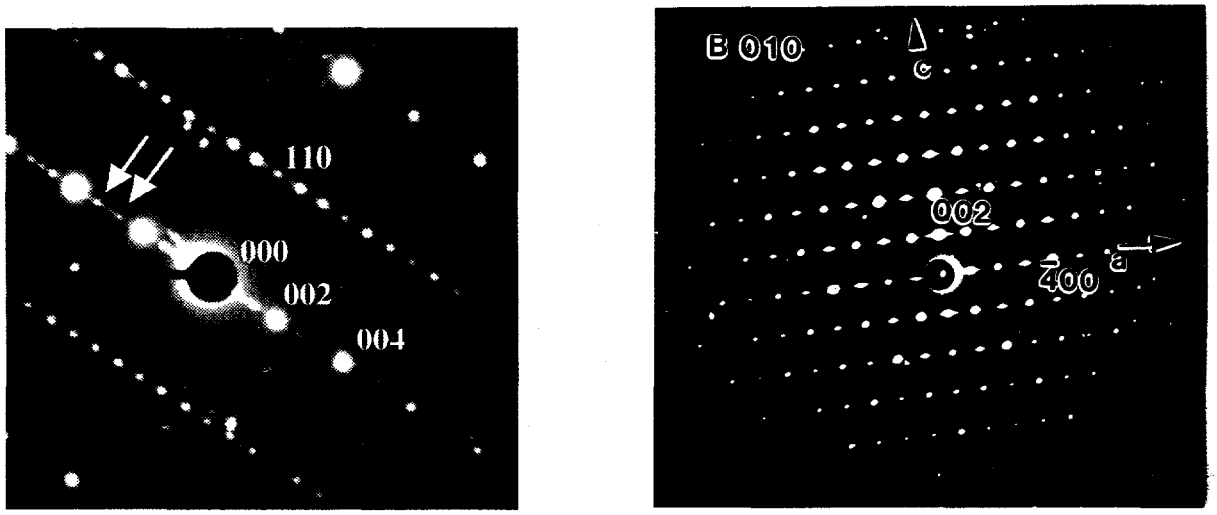

Fig. 3. Electron Diffraction Pattern Taken along $B[110]_c$ of a Zirconolite Polytype. Structure (a), estimated to be $Ca_{0.75}Gd_{0.2}Pu_{0.4}Zr_{0.75}Ti_{1.5}Al_{0.5}O_7$, exhibits superlattice reflections along the [001] direction (white arrows). The pattern has forbidden reflections for 00*l* where *l* is odd. A longer exposure was required to reveal the **c**/3 spots. (b) B[010] zone axis pattern from a polymignyte phase.

Trivalent rare earths and transuranics (e.g., Gd) may also form zirconolite-related structures of general formula $M_2Ti_2O_7$. Aluminum was found in several phases in minor amounts. Aluminum was found in more significant amounts in a titanium oxide phase and as aluminum oxide. It has been reported that aluminum (Al^{3+}) can readily exchange for Ti^{4+} in titanates with added charge compensating cations [8].

Determination of the Pu Oxidation State in Zirconolite

The oxidation state of the Pu in the zirconolite phase was determined with EELS to be in a reduced state with a technique described by Fortner and Buck [9]. The value obtained from the zirconolite phase indicated that the Pu was probably a mixture of Pu^{4+} and Pu^{3+}. The Pu-$N_{4,5}$ absorption edges exhibit sharp 'white line' transitions; these $4d_{3/2} \Rightarrow 5f_{5/2}$ (N_4) and $4d_{5/2} \Rightarrow 5f_{7/2}$ (N_5) transitions were used to determine the chemical state of the Pu in the zirconolite. The 'white lines' of Pu, Gd, and Ce can be seen in Fig. 2c. The ratio of N_4/N_5 absorption edges for a range of other actinide-bearing phases, as well as other Pu phases have been found to decrease with increasing 5*f*-orbital occupancy. In the plot shown in Fig. 4, the alkali tin silicate (ATS) glass was determined by optical methods [10] to contain Pu^{4+}. The Pu oxide was assumed to be in the +3.5 state, based on electron diffraction analysis of this phase; this suggested that it was Pu_4O_7, which is sometimes referred to as cubic Pu_2O_3 [11].

The oxidation state of the Ce present in the zirconolite in trace quantities (< 50 ppm) was determined with EELS to be +3.5 using the Ce-M_4/M_5 absorption edge ratio [9]. The Pu appears to be more oxidized than the Ce in the zirconolite. Fairly oxidizing conditions are required to move Ce into +4 state; therefore, it is expected that the Pu will have a higher average oxidation state than the Ce. However, Ce is still an effective analogue for Pu in zirconolite, as it can substitute into the same sites as the Pu.

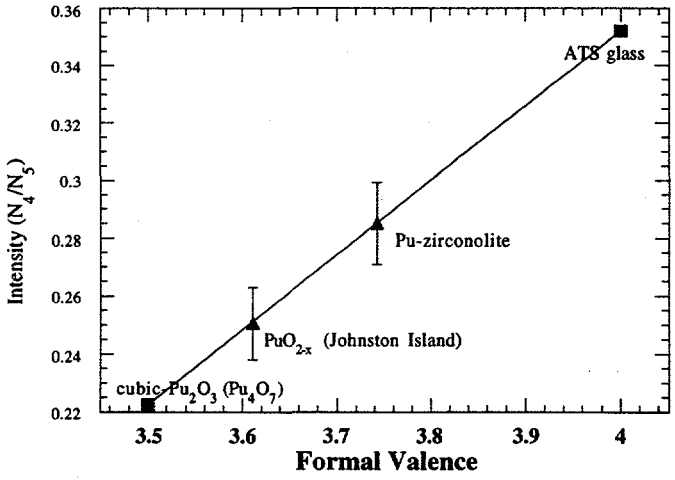

Fig. 4b. The Pu Valence in the MD Ceramic was Determined using the Ratio of the Intensity of the N_4 to N_5 White Lines. The reference data points used were the ATS glass for the Pu^{4+} [10] and the reduced plutonium oxide present in the ceramic waste form. The N_4/N_5 ratio from a partially reduced plutonium oxide obtained from a contaminated soil from Johnston Island is also shown for comparison [14]. Although this procedure apparently allows determination of the Pu oxidation state, the $N_{4,5}$ edges are complicated by multiple scattering, multiplet effects, and interactions between the bound states and the continuum. This method, therefore, requires further investigation before it can be used routinely for determination of the Pu oxidation state.

Separation of Gd and Pu in the MD Ceramic

The formulation of the MD ceramic was designed to incorporate both Gd and Pu in the zirconolite-based phases [5]. However, several phases were identified, apart from the occurrence of undissolved Pu oxide, where Gd and Pu were not associated in the same phase (see Fig. 5a). Electron diffraction analysis of a Gd-bearing calcium titanate phase suggested that it was a cubic perovskite. The introduction of Gd into this structure may have induced stabilization of this symmetry which is otherwise orthorhombic. Perovskite is known to be the least durable of the ceramic phases [3]. Brannerite phases (UTi_2O_6 and $ThTi_2O_6$) [12] have also been observed in some formulations [13]. Therefore we might expect similar Pu-bearing titanate phases to occur in the MD ceramic. Indeed, a plutonium titanate phase was identified (see Fig. 5b).

TESTING

Solution results from PCT-A are useful for comparing the reactivities of various waste forms. One of the goals of the MD program is to compare the reactivity of the Pu-ceramic to the reactivity of Pu-glasses. However, this comparison is difficult because the major components of glass (boron and silicon) are not present in the ceramic and the major components of Pu-ceramic (calcium, zirconium and titanium) are not present as major components in the Pu-glasses. In this section we will present normalized loss data for Al, Ba, Ca, Ti, and Zr. We propose that zirconium is released exclusively from zirconolite, while Ti, Al, Ba, and Ca may be released from multiple phases.

Normalized mass loss, NL(i), values (Table II) were calculated based on the mass of each element in the leachate and "acid strip" solutions, the composition of the ceramic, and the assumed S/V (2000 m^{-1}).

The particularly low values of NL(Zr) indicate that zirconolite is dissolving at a very low rate in these tests. The similar values of NL(Al) and NL(Ca) indicate that some phase containing both elements is dissolving at a significantly higher rate than the zirconolite. The relatively high NL(Ba) value shows that some relatively soluble barium phase is present in the ceramic. The NL(Ba) gives an indication of the dissolution rate of the most soluble component, and the NL(Zr) gives an indication of the solubility of the zirconolite in the ceramic.

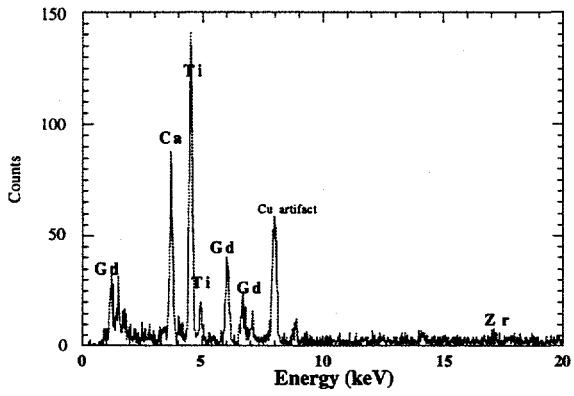

Fig. 5a. Compositional Analysis of Perovskite-Type Particle.

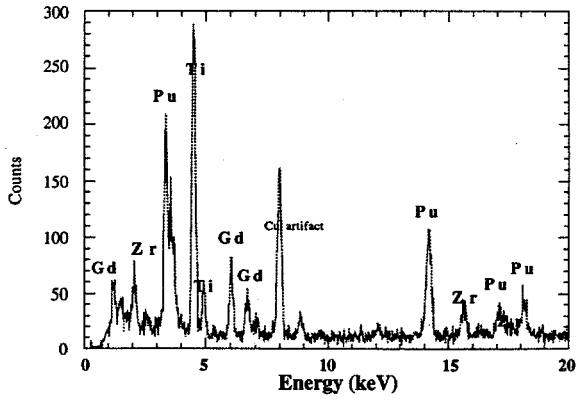

Fig. 5b. Compositional Analysis of a Pu-Titanate Phase.

Table II. Normalized Mass Loss Values for Major Components from Triplicate PCT-A with the Pu-Doped Ceramic

Element	Normalized Mass Loss (g/m^2)[a]	σ Normalized Mass Loss
Al	0.0048	0.0008
Ba	0.092	0.005
Ca	0.0059	0.0006
Ti	$<7.8x10^{-7}$ [b]	—
Zr	$<1.5x10^{-5}$ [b]	—

[a]Average of triplicate PCT-A.

[b]The normalized mass loss values are derived from limits of quantification and are therefore maximum values.

EXAMINATION OF CORRODED MD CERAMIC

The MD ceramic, reacted under vapor conditions for 35 days at 200°C, exhibited some surface alteration. In Figs. 6a,b the TEM images of the corroded surface of the ceramic show the formation of a 100-200 nm thick layer of altered material, including a region which has become enriched in Pu. The ceramic appears to have been in contact with an iron-bearing material, either from the test vessel or from contaminant iron in the ceramic.

The identification of Pu-rich regions on the outer corrosion rind in Fig. 6a suggests that dissolution of the ceramic has occurred, whereas in Fig. 6b the iron-bearing material has precipitated on the zirconolite and there is little evidence of zirconolite dissolution.

CONCLUSIONS

The characterization of the MD ceramic will continue as additional samples are received from LLNL. Knowledge of the phase distribution in the ceramic waste form is critical for understanding the results from the corrosion tests on this material. We have shown that the ceramic contains about 10-20 vol% of phases other than zirconolite or plutonium oxide, although the formulation conditions have not, as yet, being optimized for the MD ceramic. In the case of any titanate-based heterogeneous ceramic waste form, the selection of a marker element for

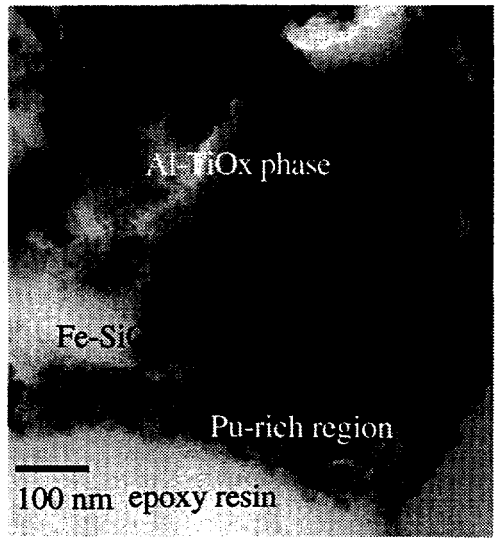

Fig. 6a. Micrographs of Al-Bearing Titanate Phase with a Surface Alteration Phase.

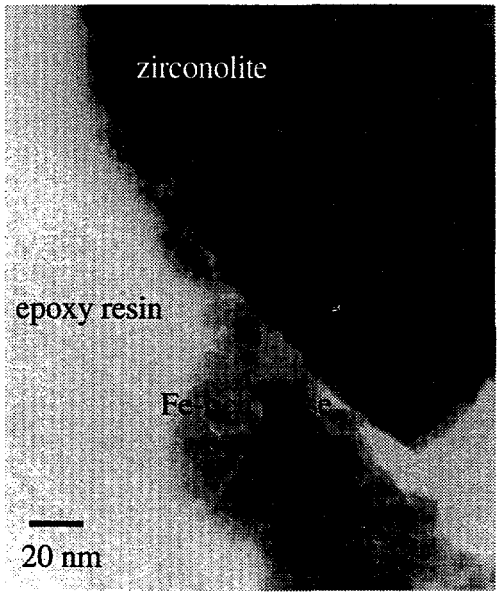

Fig. 6b. Zirconolite Crystal with Precipitated Material on Surface.

monitoring dissolution will be difficult, unless the phase distribution in the particular waste form is known. As we are interested in the corrosion of the Pu-bearing phase, which is structurally and compositionally related to zirconolite ($CaZrTi_2O_7$), we could choose Ca or Zr as a marker element. However, no single element is unique to any one phase; indeed, even plutonium is present in a number of different phases. The use of Ca to monitor the corrosion rate of the ceramic may not provide the correct data on the dissolution term. In addition, Gd and Pu do not always appear to follow each other into the different phases in the MD ceramic, and this may impact criticality assessments. In some cases, Gd is concentrated and in others Pu is concentrated. Lastly, a significant amount of the Pu is still present as an oxide, which suggests that finer PuO_2 should be used or a more reactive form such as $Pu(NO_3)_4$ be used. It is evident that a detailed TEM study will be required of any formulated ceramic to interpret corrosion testing results.

ACKNOWLEDGMENTS

This work was supported by the U.S. Department of Energy, Office of Materials Disposition, under contract W-31-109-ENG-38. Assistance in handling of the Pu ceramic was provided by J. Emery for testing, and analysis with ICP-MS was provided by S. F. Wolf and M. T. Surchik. Samples for TEM analysis were prepared by T. DiSanto.

REFERENCES

1. V. M. Oversby and W. E. Ringwood, "Leaching Studies on Synroc at 95° and 200°C," Rad. Waste Mgmt. 2, 223-237 (1982).
2. G. R. Lumpkin and R. C. Ewing, "Geochemical Alteration of Pyrochlore Group Minerals: Pyrochlore Subgroup," Am. Miner. 80, 732-743 (1995).
3. P. J. McGlinn, K. P. Hart, E. H. Loi, and E. R. Vance, "pH Dependence of the Aqueous Dissolution Rates of Perovskite and Zirconolite at 90°C," Mater. Res. Soc. Symp. Proc. 353, 847-854 (1995).
4. R. A. Van Konynenburg and M. W. Guinan, *Plutonium Doping of Synroc-D*, Lawrence Livermore National Laboratory Report UCRL-53425 (1983).
5. E. R. Vance, C. J. Ball, R. A. Day, K. L. Smith, M. G. Blackford, B. D. Begg, and P. Angel, "Actinide and Rare Earth Incorporation into Zirconolite," J. Alloys Comp. 213/214, 406-409 (1994).
6. *Standard Test Methods for Determining Chemical Durability of Nuclear Waste Glasses: The Product Consistency Test (PCT),* ASTM Standard C1285-94, ASTM, Philadelphia PA (1994).
7. D. J. Wronkiewicz, L. M. Wang, J. K. Bates, and B. S. Tani, "Effects of Radiation on Glass Alteration in a Steam Environment," 294, 183-190 (1993).
8. T. J. White, "The Microstructure of Synthetic Zirconolite, Zirkelite, and Related Phases," Am. Miner. 69, 1156-1172 (1984).
9. J. A. Fortner and E. C. Buck, "The Chemistry of the Light Rare-Earth Elements as determined by Electron Energy Loss Spectroscopy," Appl. Phys. Lett. 68, 3817-3819 (1996).
10. L. Nuñez and J. A. Fortner, Argonne National Laboratory, private communication (1996).
11. R. B. Roof, *X-ray Diffraction Data for Plutonium Compounds*, Los Alamos National Laboratory Report LA-11619 (1989)
12. R. Ruh and A. D. Wadsley, "The Crystal Structure of $ThTi_2O_6$ (Brannerite)," Acta Cryst. 21, 974-978 (1966).
13. E. R. Vance, P. J. Angel, B. D. Begg, and R. A. Day, "Zirconolite-Rich Ceramics for High-Level Actinide Wastes," Mater. Res. Soc. Symp. Proc. 333, 293-298 (1994).
14. S. F. Wolf, N. R. Brown, J. A. Fortner, E. C. Buck, N. L. Dietz, and J. K. Bates, Environ. Sci. Technol. 31 (1997).